CCC Meeting

August 16, 2012

Modeling crystallization process of mold slag

Lejun Zhou

Advisors: Prof. Brian G. Thomas and Wanlin Wang

Department of Mechanical Science & Engineering
University of Illinois at Urbana-Champaign

School of Metallurgical Science and Engineering
Central South University

Background

- The significant important functions of mold slag in continuous casting of steel

  -Protecting the steel from oxidation, insulating the steel from freezing and absorbing inclusions.

  -Lubricating the shell and moderating the heat transfer in the mold, which is greatly affected by the slag crystallization properties

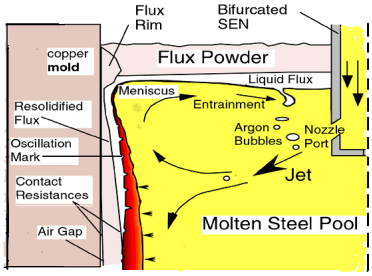

Fig.1 schematic of inner mold [1]

- Investigation of mold slag crystallization by using Double Hot Thermocouple Technology (DHTT) and Single Hot Thermocouple Technology (SHTT)
  - Favored by many other researchers due to its visual as well as high heating and cooling rates [2-3].
  - Temperature may vary within the sample during the measurement process, it is only known at thermocouples at 1-2 locations.

Experiment-SHTT

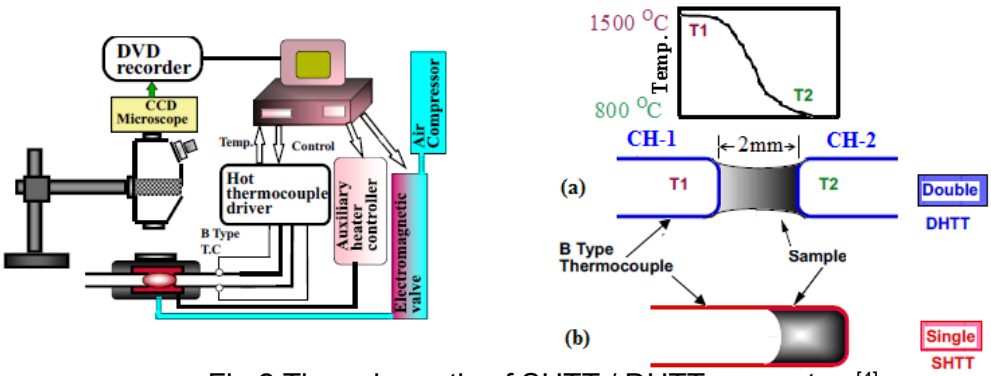

Fig.2 The schematic of SHTT / DHTT apparatus [4]

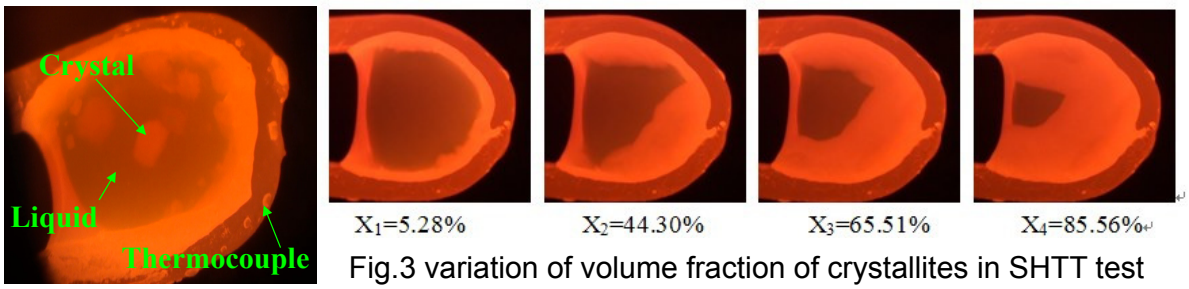

Fig.3 variation of volume fraction of crystallites in SHTT test

Experiment-DHTT

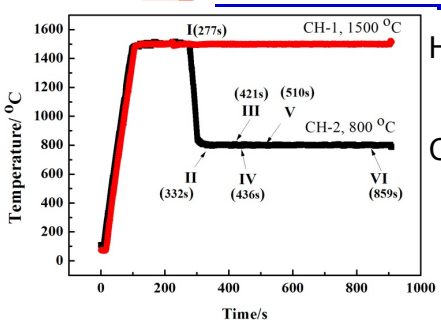

Hot TC(CH-2)

Cold TC (CH-1)

Stage 1(preheating) Stage 2 (quenching)

Stage 3 (holding)

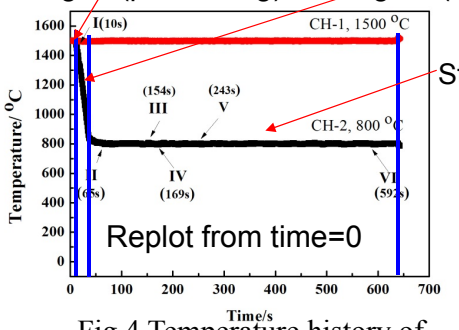

Fig.4 Temperature history of DHTT for LC mold flux

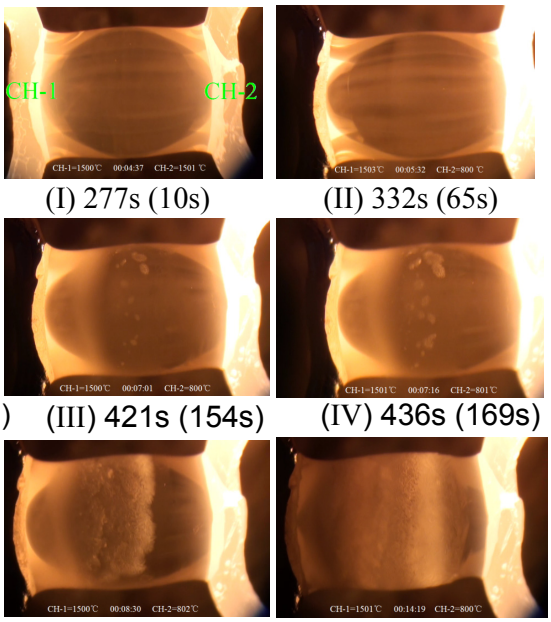

(I) 277s (10s) (II) 332s (65s)

(III) 421s (154s) (IV) 436s (169s)

(V) 510s(243s) (VI) 859s (592s)

Fig.5 evolution of crystalline layer in DHTT experiment

Objectives

- To develop a computational models of DHTT experiment, including heat transfer, fluid flow, and crystallization of mold slag
- To investigate the interaction between temperature variations in the mold slag and crystallization
- To determine the effect of Marangoni flow and natural convection phenomena in the experiment

Geometry / Simulation Domain of DHTT

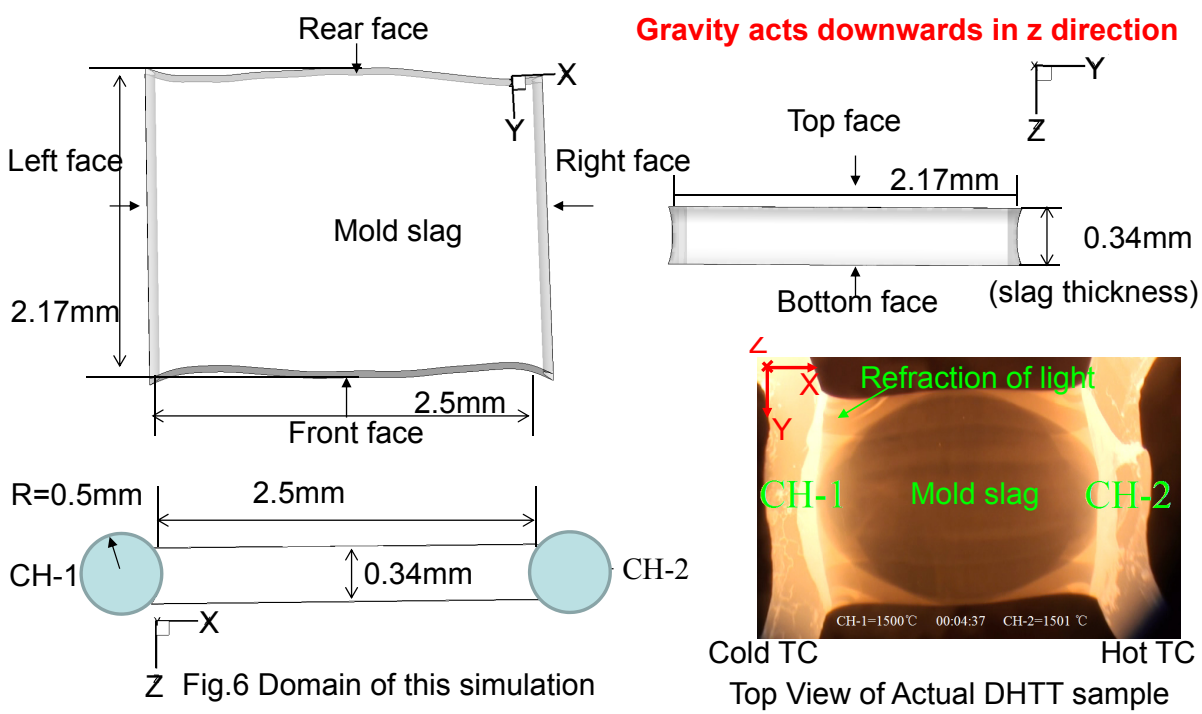

Fig.6 Domain of this simulation

Top View of Actual DHTT sample

Governing equations

Part 1: Heat transfer model

$$\frac{\partial}{\partial t}(\rho E)+\nabla\cdot(\vec{v}(\rho E))=\nabla\cdot(k_{eff}\nabla T)+S_h$$

Source term: $S_h=\frac{H_{latent\,heat}}{\rho\cdot C\_Volume}$

Part 2: Fluid flow model

$$\frac{\partial}{\partial t}(\rho\vec{v})+\nabla\bullet(\rho\vec{v}\vec{v})=-\nabla p+\nabla\bullet(\bar{\bar{\tau}})+\rho\vec{g}$$

The buoyancy effect is included through the term in the gravity direction (Z axis direction in figure 5).And, the boussinesq approximation is:

$$\rho=\rho_0(1-\beta\Delta T)$$

ρ_0 is the density at operation temperature

β is the thermal expansion coefficient of mold slag

Governing equations

Part 3: Isothermal crystallization model

Johnson-Mehl-Avrami (JMA) equation

$$X=1-\exp\{-[k(t-\tau)]^n\}$$

Because of the impossible of getting the actual incubation time directly from the SHTT experiment, thus:

$$\ln\ln\left(\frac{1}{1-X^*}\right)=n\ln k+n\ln(t-\tau^*)$$ → Obtain n and k

Where, $X^*=X-X_{0.05}$ $\tau^*=\tau_{0.05}$

X is the actual crystalline fraction, $X_{0.05}$ is the crystalline fraction=0.05.

τ is the actual incubation time, before that nucleation rate is zero.

$\tau_{0.05}$ is the corresponding time when crystalline fraction is 0.05.

$$\ln\ln\left(\frac{1}{1-X_{0.05}}\right)=n\ln k+n\ln(\tau_{0.05}-\tau)$$

→ Obtain temperature dependent τ

Assumption:

If $t\geq\tau$ → UDM=1(crystal)

If $t<\tau$ → UDM=0 (liquid)

Crystallization equation from isothermal-cyst. SHHT results

Table 1 mineral percentage of the mold fluxes used in this study

	CaO	SiO_2	Al_2O_3	MgO	CaF_2	Na_2O	Li_2O
Mass%	25.11	41.54	7.06	2.03	12.09	9.20	0.49

Table 2 mineral percentage of the other mold fluxes used in figure 12

	CaO	SiO_2	Al_2O_3	MgO	CaF_2	Na_2O	Li_2O
Mass%	37.73	32.86	12.08	2.02	8.05	5.11	0.50

Note: Mold slag in Table 1 was chosen over the composition in Table 2 because: Table 2 slag crystallizes very fast, so is harder to measure.

Crystallization equation from isothermal-cyst. SHTT results

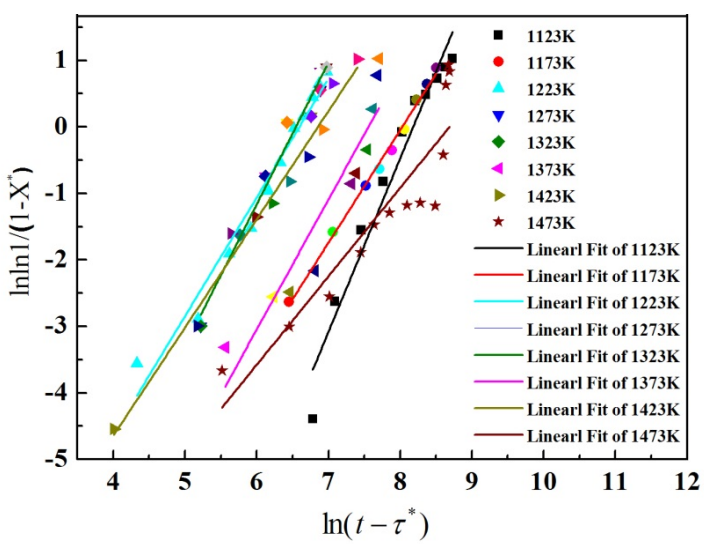

Fig.7 The relation of crystalline fraction evolution with function of time

Temperature, K	n	lnk
1123	2.62	-8.18
1173	1.92	-7.55
1223	1.76	-6.69
1273	2.13	-6.55
1323	1.31	-5.88
1373	1.96	-7.54
1427	2.49	-6.85
1473	1.33	-8.69

Table 3 the values of n and k at different temperature

Crystallization equation from isothermal-cyst. SHTT results

Table 4 the incubation time at different temperature

Temperature, K	1123	1173	1223	1273	1323	1373	1427	1473
Incubation time, s	246	155	105	172	190	233	310	442

$$\tau = f(T) = A_0 + A_1 T + A_2 T^2 + A_3 T^3 + A_4 T^4 + A_5 T^5$$

Where, A_0= 1.47, A_1=379.58093, A_2= -1.15396779, A_3=0.00131489225, A_4=-6.65604E-07 , A_5=2635228E-10

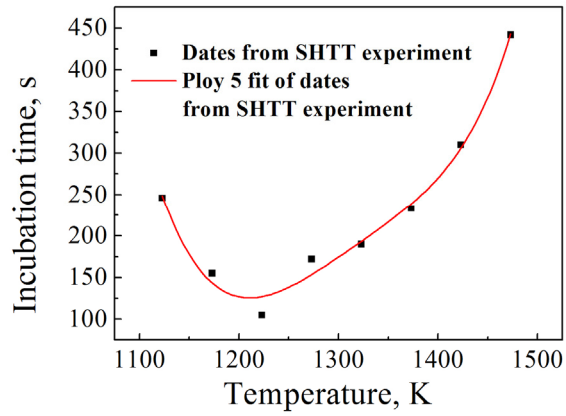

Fig.8 The temperature dependent of incubation time →

Boundary conditions

Thermal boundary conditions

	Stage 1	Stage 2 30k/s	Stage 3 Holding
Left face:	$T_L = 1773K(1500\ ^oC)$	$T_L = 1773K(1500^oC) \longrightarrow 1073K(800\ ^oC) \longrightarrow$	
Right face:	$T_{Ri} = 1773K(1500\ ^oC)$	←	←
Front face:	$q_F = \varepsilon \cdot \sigma \cdot (T_F^4 - T_{air}^4) = q_c = K_{eff} \cdot \frac{dT}{dy}$	←	←
Rear face:	$q_{Re} = \varepsilon \cdot \sigma \cdot (T_{Re}^4 - T_{air}^4) = q_c = K_{eff} \cdot \frac{dT}{dz}$	←	←
Top face:	$q_T = \varepsilon \cdot \sigma \cdot (T_T^4 - T_{air}^4) = q_c = K_{eff} \cdot \frac{dT}{dz}$	←	←
Bottom face:	$q_B = \varepsilon \cdot \sigma \cdot (T_B^4 - T_{air}^4) = q_c = K_{eff} \cdot \frac{dT}{dz}$	←	←

Fluid boundary condition

Marangoni stress: $\tau = \frac{d\gamma}{dT} \bullet \frac{\partial T}{\partial r}$ γ is the surface tension

Material properties

Thermal & fluid properties

Thermal Properties	Value
Cp (J/kg·k)	$1.1\times10^{3}+6.3\times10^{-2}T-3.5\times10^{-7}/T^{2}$ [8]
Latent heat(J/Kg)	6.1×10^{5} [8]
Effective Thermal Conductivity (W/m·k)	Liquid: 3 [9-10] Crystalline: 1.7
Emissivity	0.8 [9,12,13]
Fluid Properties	
Viscosity (kg/m·s)	-8.194+11989.17/T [11]
Density (kg/m3)	3021-0.33T [5-7]
Surface tension, (mN/m)	624.33-0.12T [14-15]
Surface tension gradient with temp (N/m-K)	-0.00012

Temperature distribution –stage1

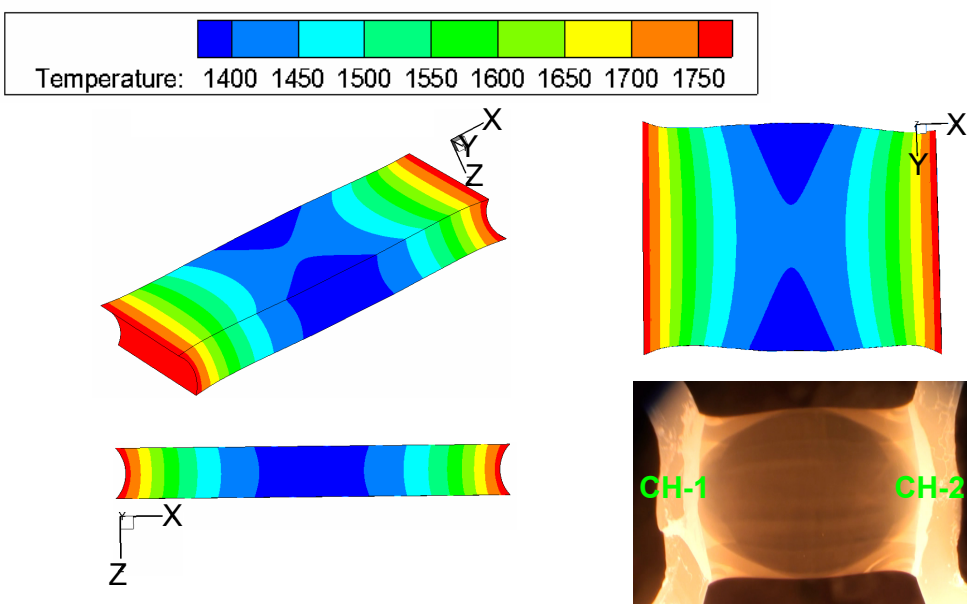

Fig. 9 Temperature contours after the TC-1=1773K (1500 ^{O}C) and TC-2=1773K (1500 ^{O}C) reaching steady state

Temperature distribution –stage1

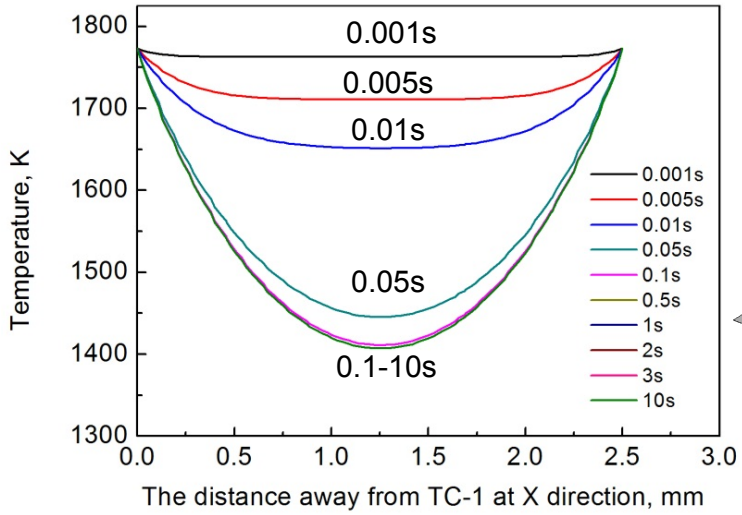

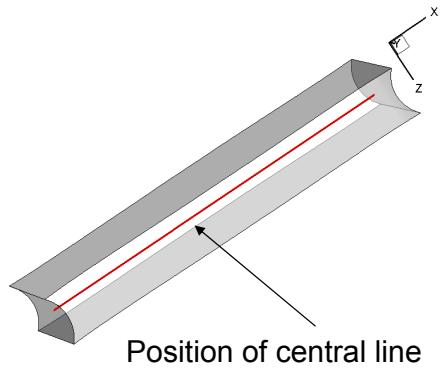

Fig. 10 Temperature distribution at the central line

Note: 1) Radiation cooling causes lower temperature in central region.
2) Time needed for thermal steady state is short because sample is very thin.

Fluid flow distribution –stage1

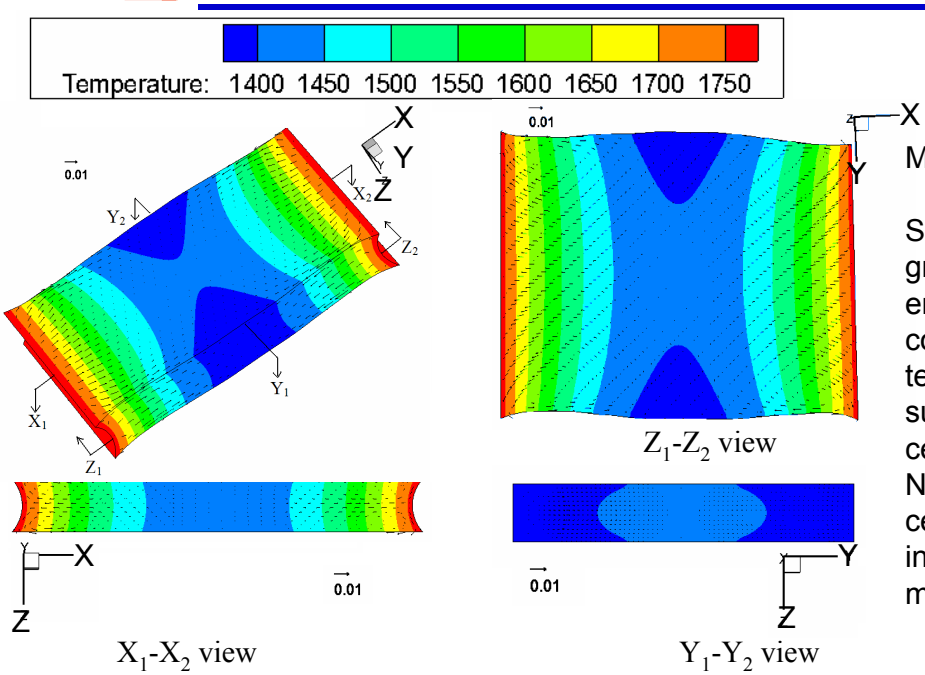

Marangoni flow:

Surface-tension gradient from hot ends (low tension) to cold center (high tension) pulls surface flow towards center.
Note return flow from center to ends in the interior, to conserve mass.

Fig. 11 fluid flow after the TC-1=1773K and TC-2=1773K reach steady state

Fluid flow distribution –stage1

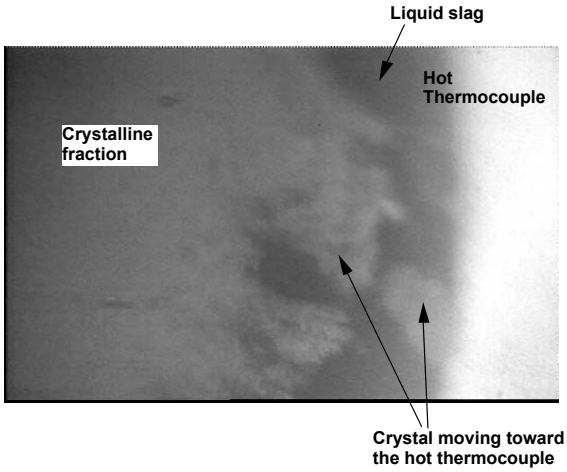

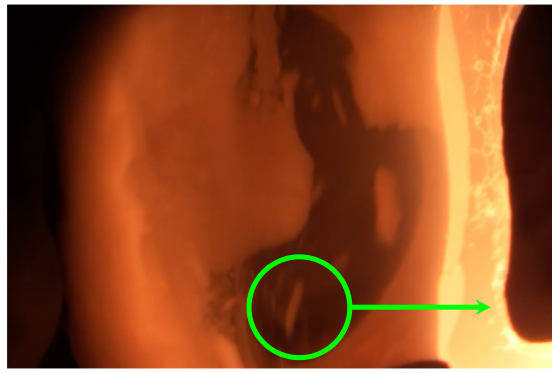

Observed by Prof. Cramb[2]

Observed In Our lab

Fig. 12 Crystals separate and move with flow in liquid

Reasons : Crystals move by Marangoni and natural convection flow.
Crystals difficult to precipitate near hot TC.

Fluid flow distribution –stage1

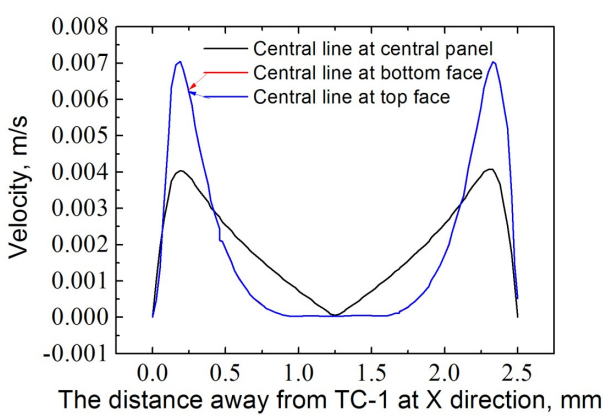

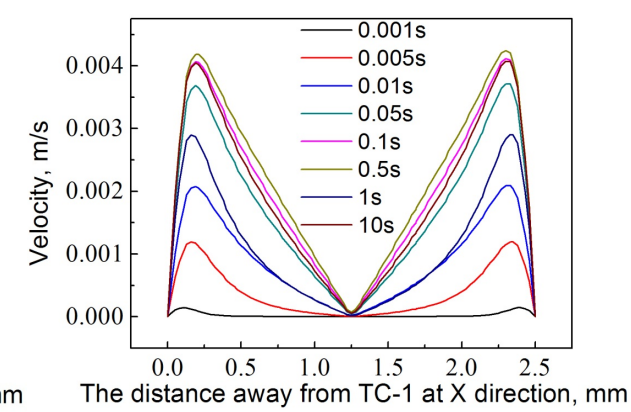

Fig.13 velocity magnitude of central line at top, bottom faces and central panel at t=10s

Fig.14 velocity magnitude of central line at central panel

- Velocity on the surface is larger than in interior of mold slag.
- The largest velocity occurred at 0.5s and the smallest occurred at 0.001s

Temperature distribution –stage 2 and 3

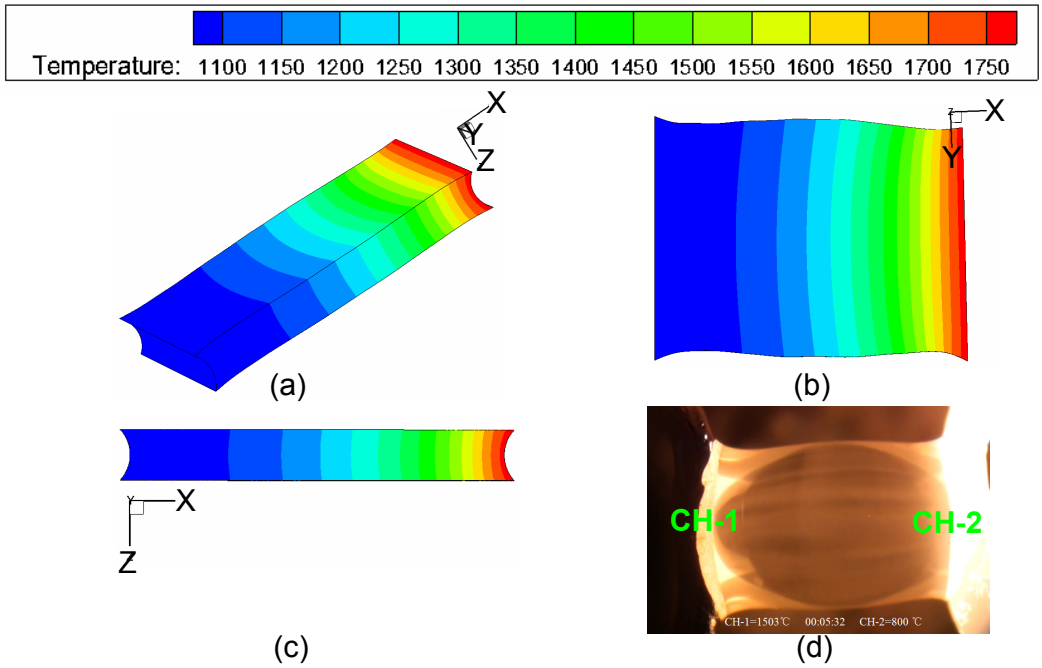

Fig. 15 temperature contours after the TC-1 cooled to 1073K (800 ^{O}C)

Temperature distribution –stage 2 and 3

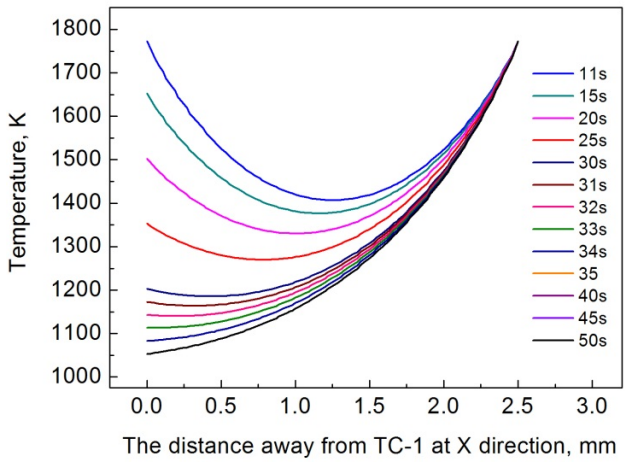

Fig. 16 temperature distributions in X direction

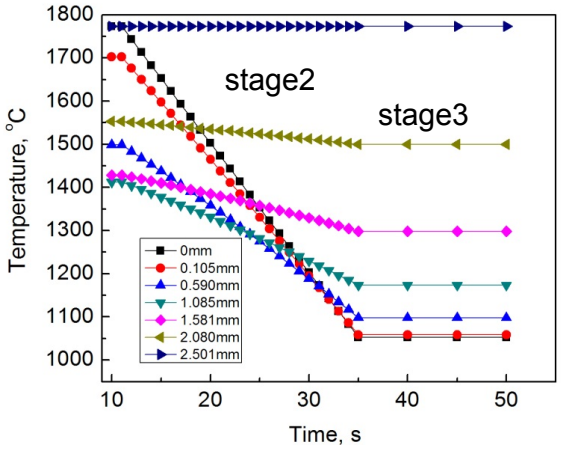

Fig.17 the temperature variation with time

Temperature at different location decreasing with TC-1 cooling down during stage 2 Then, it keeps steady state before the precipitation of crystal layer.

Temperature distribution –stage 2 and 3

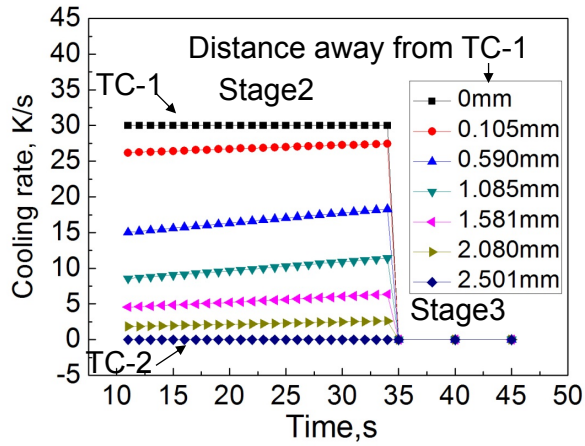

Fig. 18 the cooling rate variation with time at different position

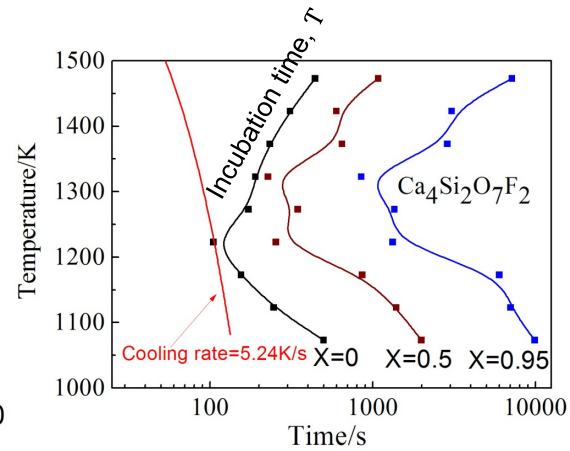

Fig. 19 TTT diagram of mold slag

- Cooling rate is max at cold TC-1, and decreases to zero at hot TC-2 .
- If cooling rate exceeds critical, glassy phase may form.
- Quenching is interrupted before glass can form, allowing crystallization

Temperature distribution –stage 2 and 3

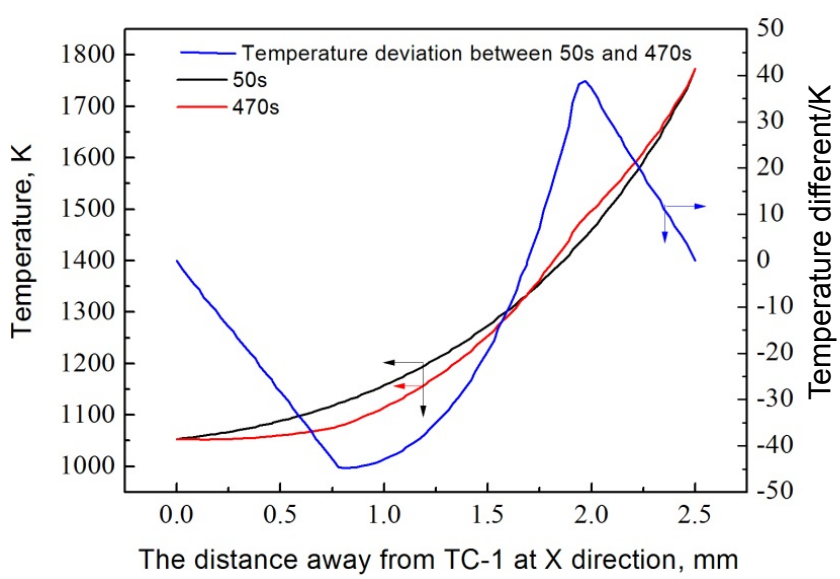

Fig. 20 the cooling rate variation with time at different position

Precipitation of central crystalline layer lowers the heat flux from hot TC to cold TC.

This causes temperature to increase near hot TC and decrease near cold TC

Fluid flow distribution –stage 2 and 3

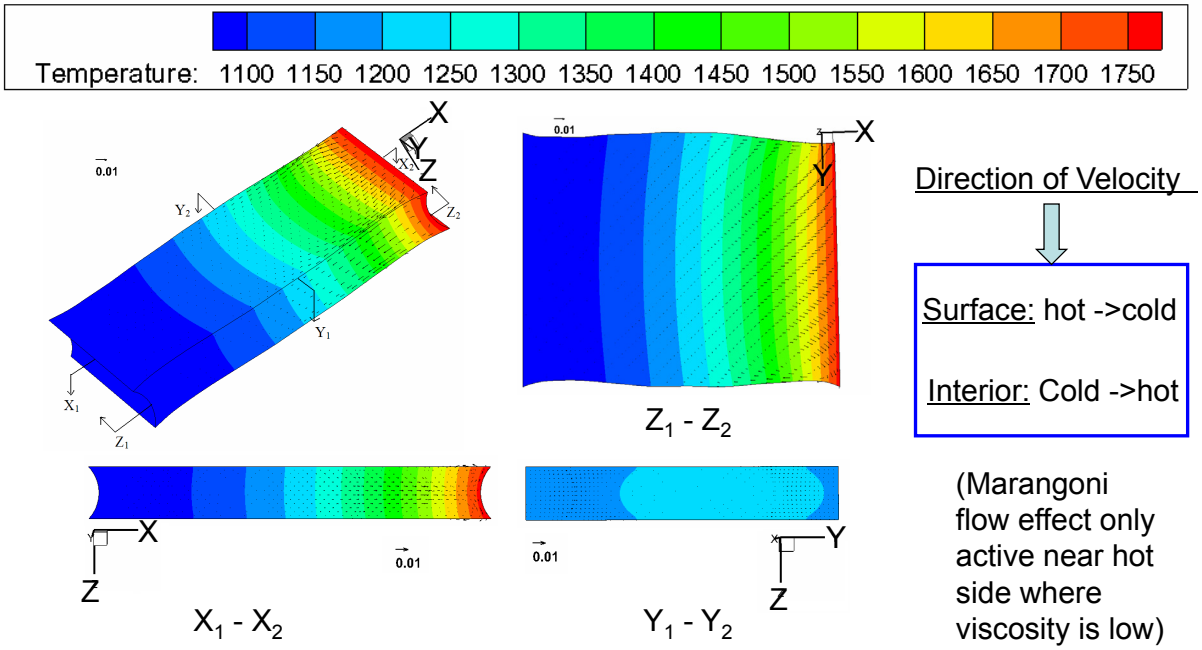

Direction of Velocity

Surface: hot ->cold

Interior: Cold ->hot

(Marangoni flow effect only active near hot side where viscosity is low)

Fig.21 Fluid flow distribution at 50s

Fluid flow distribution –stage 2 and 3

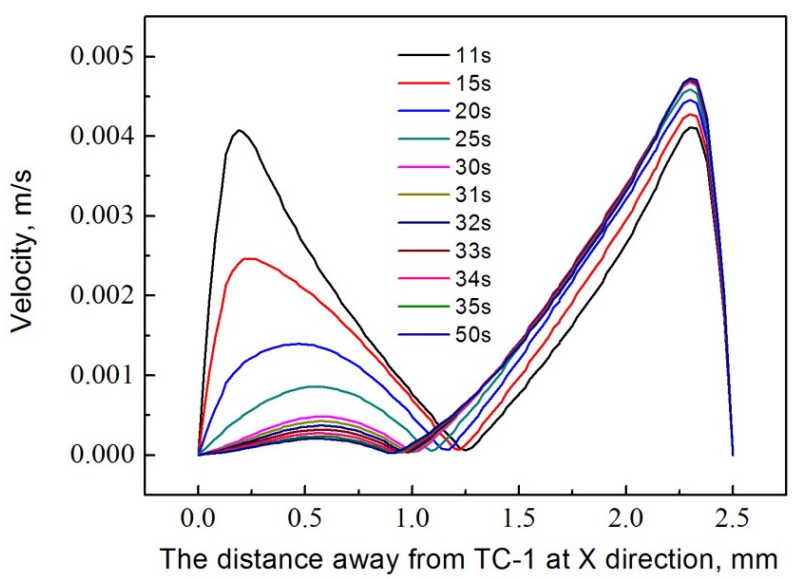

Fig. 22 velocity magnitude of central line on central panel from 11s to 50s

Crystallization Model and Validation

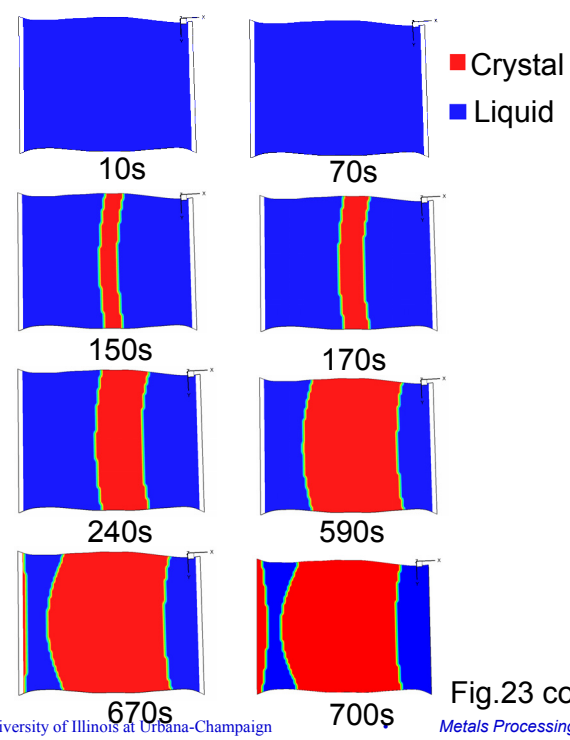

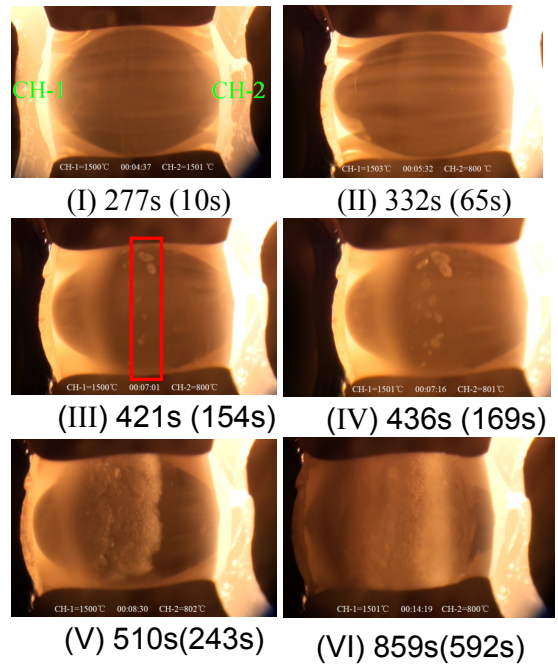

Fig.23 compare the evolution of crystallization results

Summary

- Model of heat transfer, fluid flow, and crystallization developed and applied to Mold slag crystallization during a DHTT test with stages of 1=preheat; 2=quench; 3=hold, designed to simulate slag crystallization near meniscus.
- The crystallization model (based on nucleation from SHTT results) matches well with DHTT experiments except perhaps at later stages, where neglect of growth becomes important.
- During stage 1, temperature in the middle of mold slag drops lower than both TCs, which initiates crystallization near the sample center.
- During stage2, cooling rate is max at cold TC-1 (like mold wall), and decreases to zero at hot TC-2 (like steel shell).
- Crystallization of central layer lowers conductivity, which lowers heat flux across the sample, making the hotter part hotter, and cooler part cooler.

Summary

- Fluid flow recirculates from the hot TC2 to the cooler center along the surface; and then flow from the cooler central region to the hot TC-2 region through the interior of the mold slag sample, driven by Marangoni flow, which matches the observations of crystal movement.
- Natural convection effects seem small.
- Experimentalists need to consider the non-uniform temperature & flow effects during their slag crystallization experimental analysis.
- Future work: use this experiment and analysis to study slag formation in gap, where hot TC-2 temperature drops with time (as slag moves down mold).

References

[1] Brian G. Thomas, Modeling of the continuous casting of steel-past, present and future. Brimacombe Lecture, 59 th Electric Furnace of Conf., Pheonix, AZ, 2001, Iron & steel Soc., pp.3-30
[2] A. W. Cramb: Report: American Iron and Steel Institute, Technology Roadmap Program, Pittsburgh, PA, USA, 2003)
[3] G. Wen, H. Liu and P. Tang: J. Iron Steel Res. Int., 2008, vol.15 (4): pp.32-37
[4] Y. Kashiwaya, C. E. Cicutti, A. W. Cramb and K. Ishii: ISIJ Int., 1998, 38(4), pp. 348-356
[5] Ken Mills. The estimation of slag properties. Southern African Pyrometallurgy, 2011, p:1-49
[6] S. A. Nelson and I.S.E. Carmichael. Partial molar volumes of oxide components in silicate liquids. Contributions to Mineralogy and Petrology, 1979, (71), pp.117-124
[7] Christian Robelin and Patrice Chartrand. A density model based on the modified quasichemical model and applied to the NaF-AlF3-CaF2-Al2O3 electrolyte. Metallurgical and Materials Transactions B, 2007, 38B, pp.881-892
[8] Dalun Ye, Jianhua Hu. handbook of thermodynamic data for Inorganic Materials, Beijing: Metallurgical industry press. 2002.
[9] R.M. McDavid and B.G. Thomas. Flow and thermal behavior of the top surface flux/powder layers in continuous casting molds. Metallurgical and materials transaction B, 1996, 27B: 672-685
[10]KEZHUAN GU, WANLIN WANG, LEJUN ZHOU, FANJUN MA, and DAOYUAN HUANG. The Effect of Basicity on the Radiative Heat Transfer and Interfacial Thermal Resistance in Continuous Casting. Metallurgical and Materials Transactions B. Oline First, 8 Mach, 2012
[11] K.C. Mills and S. Sridhar. Viscosity of ironmaking and steelmaking slags. Ironmaking and Steelmaking, 1999, 26 (4): 262
[12] Viswanathan Nurni Neelakantan, Seetharaman Sridhar, K. C. Mills and Du Sichen. Mathematical model to simulate the temperature and composition distribution inside the flux layer of a continuous casting mould. Scandinavian Journal of Metallurgy, 2002, Vol.31 (3), pp. 191–200
[13] YA MENG and BRIAN G. THOMAS. Heat-Transfer and Solidification Model of Continuous Slab Casting: CON1D. Metallurgical and Materials Transactions B, 2003, Vol.34B, pp.685-705.
[14]Masahito HANAO etc. Evaluation of surface tension of molten slag in multicomponent systems. ISIJ International, Vol.47(2007), No.7,pp.935-939
[15] K. C. Mills and Y. C. Su. Review of surface tension data for metallic elements and alloys part 1-pure metals. International materials reviews, 2006, 50 (6):329-351

Acknowledgements

- Continuous Casting Consortium Members (ABB, ArcelorMittal, Baosteel, Tata Steel, Goodrich, Magnesita Refractories, Nucor Steel, Nippon Steel, Postech/ Posco, SSAB, ANSYS-Fluent)

- Prof.Brian,G.Thomas and other people in CCC research group

- Prof. Wanlin Wang, CHINA SCHOLARSHIP COUNCIL, International Science & Technology Cooperation Program of China (2011DFA 71390)